On the Doppler Spreading Effect for the Range-Instantaneous-Doppler Technique in Inverse Synthetic Aperture Radar Imagery

J. M. Muñoz-Ferreras and F. Pérez-Martínez

***Abstract*—Inverse synthetic aperture radar (ISAR) is an all-weather radar technique which may generate high-resolution images of noncooperative targets. The standard range-Doppler algorithm (RDA) is usually employed for image generation. However, the images obtained with RDA are usually blurred because of the relative motion between radar and target. As a consequence, motion compensation techniques should be used to improve the imagery quality. The range-instantaneous-Doppler (RID) technique based on time–frequency transforms has been proposed for obtaining a sequence of focused ISAR images without the need of using motion compensation techniques. However, in this letter, it is clearly shown that the migration of the target scatterers in slant range indirectly induces Doppler spreading of the scatterers' point spread function in each of the ISAR images obtained by the RID technique. This Doppler spreading means blurring. It is important to highlight that the migration in slant range may be caused not only by the radial component of the translational motion but also by the rotational motion. The application of motion compensation techniques prior to the use of the RID technique allows us to mitigate the Doppler spreading, as shown here both for simulated and live data acquired by a high-resolution coherent radar.**

***Index Terms*—Doppler spreading, inverse synthetic aperture radar (ISAR), motion compensation, noncooperative targets, range-instantaneous-Doppler (RID) technique.**

I. Introduction

INVERSE synthetic aperture radar (ISAR) imaging is a coherent radar technique which generates range-Doppler images of noncooperative targets [1], [2]. The ISAR technique is usually considered as a complement for other image generator sensors, such as passive cameras or laser radar systems [3], [4], which may have a reduced performance in adverse meteorological conditions, like fog.

In the standard ISAR scenario of a static radar illuminating a maneuvering target, a high slant-range resolution is obtained by transmitting a large bandwidth signal, whereas a high cross-range resolution depends on a large variation of the target aspect angle during the coherent processing interval (CPI) [5]. The standard range-Doppler algorithm (RDA) generates the ISAR image by applying a fast Fourier transform in each range bin, once a stack of range profiles has been obtained [5].

Manuscript received December 9, 2008; revised July 17, 2009. First published October 2, 2009; current version published January 13, 2010. This work was supported by the Spanish National Board of Scientific and Technology Research under Projects TEC2005-07010-C02 and TEC2008-02148/TEC.

J. M. Muñoz-Ferreras is with the Department of Signal Theory and Communications, University of Alcalá, 28805 Madrid, Spain.

F. Pérez-Martínez is with the Department of Signals, Systems and Radiocommunications, Technical University of Madrid, 28040 Madrid, Spain.

Digital Object Identifier 10.1109/LGRS.2009.2030372

Target motion may be divided into a translational component and a rotational component. The line-of-sight (LOS) projection of the translational motion does not induce aspect angle change. Moreover, it produces large blurring. The tangential projection (across LOS) of the translational motion and the rotational motion (yaw, pitch, and roll) may generate aspect angle change and, as a consequence, the desired Doppler gradient among target scatterers situated in the same range bin. However, these components may also produce blurring: migration through resolution cells (MTRC) [6].

Hence, if no motion compensation techniques are applied, the ISAR images obtained with RDA are usually blurred. Translational motion compensation methods work in two steps: range bin alignment and phase adjustment. Envelope correlation [1], [7], [8], Doppler centroid tracking [9] and global range alignment [10] are some methods proposed for the first step. In the phase adjustment stage, prominent point processing [11], phase gradient autofocus [12], minimum entropy method [13], [14], maximum contrast method [15], higher order statistics autofocus [16], and so on have been addressed.

On the other hand, rotational motion compensation methods for MTRC correction are diverse: prominent point-based methods [17]–[19], the keystone formatting-based technique [20], the method based on the local polynomial Fourier transform [21], the approach based on the fractional Fourier transform [22], etc.

The range-instantaneous-Doppler (RID) technique [23]–[25] based on the use of time–frequency transforms (TFTs) has been proposed for obtaining a sequence of focused ISAR images without the need of sophisticated motion compensation techniques. However, as clearly shown in this letter, if a scatterer migrates through slant-range cells during the CPI, then Doppler spreading of its point spread function (PSF) arises for each of the ISAR images obtained by the RID technique. This Doppler spreading can be understood as blurring.

The main innovative aspects developed in this letter may be summarized as follows.

1) This letter demonstrates that the migration in slant range of the target scatterers indirectly induces Doppler spreading of their corresponding PSFs in each of the ISAR images generated by the RID technique. This Doppler spreading means a loss of quality in the RID outputs.
2) It is highlighted that the slant-range migration, which is the cause of the commented blurring, may be produced

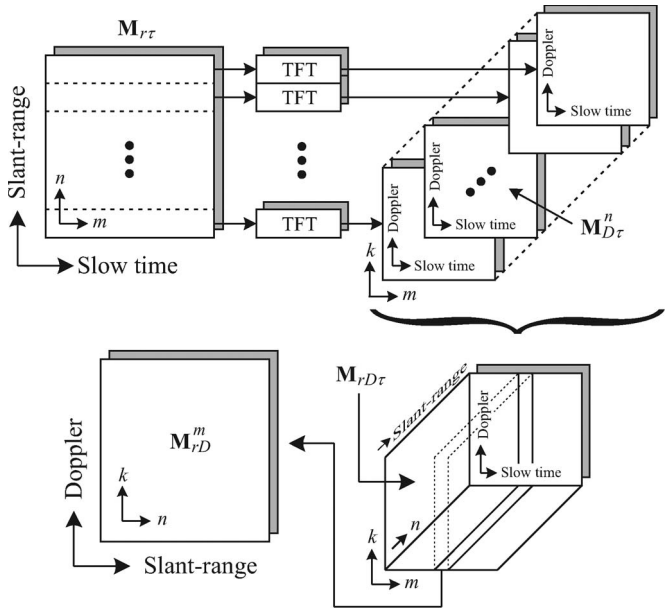

Fig. 1. Conceptual scheme of the RID technique.

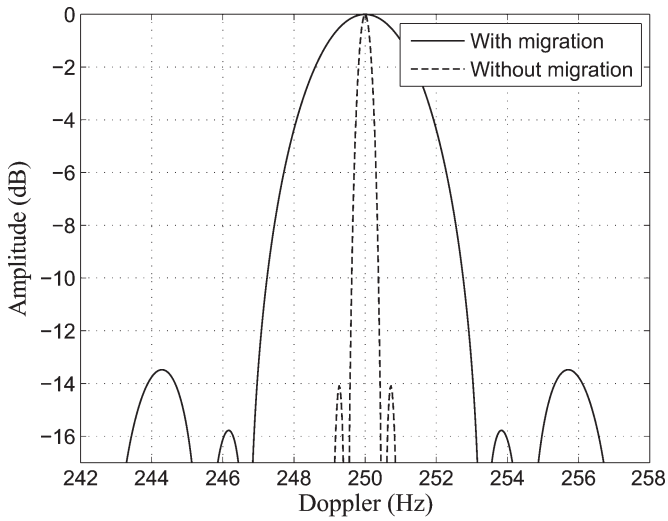

Fig. 2. Doppler spreading as a consequence of the scatterer migration in slant range, when using the RID approach. Doppler cutoff of the scatterer PSF (continuous line) with migration in slant range and (dashed line) without migration in slant range.

not only by the radial component of the translational motion but also by the components which may induce variation of the target aspect angle [the tangential component of the translational motion and the attitude components (yaw, pitch, and roll)].

3) Once the origin of the blurring is clear, the proposal of a mitigation algorithm is trivial: Motion compensation techniques must be used in order to correct the slant-range migration. This conclusion is contrary to what is claimed when using the RID technique: No motion compensation techniques are necessary. In this letter, the performance of the blurring mitigation algorithm is shown both for simulated and real data.
4) The authors admit the difficulty of compensating the rotational motion for noncooperative targets involved in complex motions and whose effective rotation vector is dynamically and quickly changing its direction. For these cases, at least, translational motion compensation should be applied prior to the RID technique. By doing this, the Doppler spreading is greatly but not completely mitigated, because the slant-range migration is, in practical cases, mainly caused by the LOS projection of the translational motion. The possible blurring residual must be found in the uncompensated slant-range migration caused by the rotational motion.

II. RID Technique and Doppler Spreading

A. RID Technique

The RID technique is based on the use of TFTs. Once some range profiles have been acquired during the CPI, a TFT is applied to each range bin. As a consequence, a 3-D range-Doppler-slow time matrix is constructed, whose slices in slow time are the sequence of ISAR images.

Fig. 1 schematically shows the processing of the RID technique. For the nth range bin of the range-slow time matrix $\mathbf{M}_{r\tau}[n, m]$, a TFT is applied to obtain the nth Doppler-slow time map $\mathbf{M}^n_{D\tau}[k, m]$. The slices of the range-Doppler-slow time parallelepiped $\mathbf{M}_{rD\tau}[n, k, m]$ in m are the focused ISAR images $\mathbf{M}^m_{rD}[n, k]$.

B. Associated Doppler Spreading

The migration of the target scatterers in slant range causes Doppler spreading of their PSFs in each of the images generated by the RID technique. To show this, we consider a simplified example.

Let us suppose a single scatterer with a Doppler frequency of 250 Hz. The CPI is 1 s, and the scatterer remains in its initial range bin (n_i) for the first $CPI/4$ s (0.25 s). Then, it changes its range cell, i.e., it moves from the n_ith range bin to the $(n_i - 1)$th or the $(n_i + 1)$th range cell at $CPI/4$ s. As a consequence, the Doppler-slow time map $\mathbf{M}^{n_i}_{D\tau}[k, m]$, corresponding to the n_ith range cell, will show a constant Doppler line (250 Hz) for the first 0.25 s. However, this line is wide in Doppler because we only have signal in the vector $\mathbf{M}_{r\tau}[n_i, m]$ for the first $CPI/4$ s. A line more concentrated in Doppler would have been obtained, if the scatterer had remained in the n_ith range bin for all the CPI, which is equivalent to the response resulting from perfect motion compensation.

Fig. 2 (continuous line) shows the Doppler cutoff of the scatterer PSF for the ISAR image at $CPI/8$ s (0.125 s) when the scatterer migrates at $CPI/4$ s, and we directly use the RID method. The dashed line in Fig. 2 refers to the same Doppler cutoff when motion has been compensated prior to applying the RID technique. In this second case, the scatterer remains in the n_ith range bin for all the CPI. The smoothed pseudo Wigner–Ville distribution (SPWVD) [26] has been used as TFT. The PSF Doppler width at -3-dB points is 3.38 and 0.61 Hz, respectively. Hence, Fig. 2 clearly shows that migration in slant range indirectly causes Doppler spreading, which degrades the quality of the obtained ISAR images.

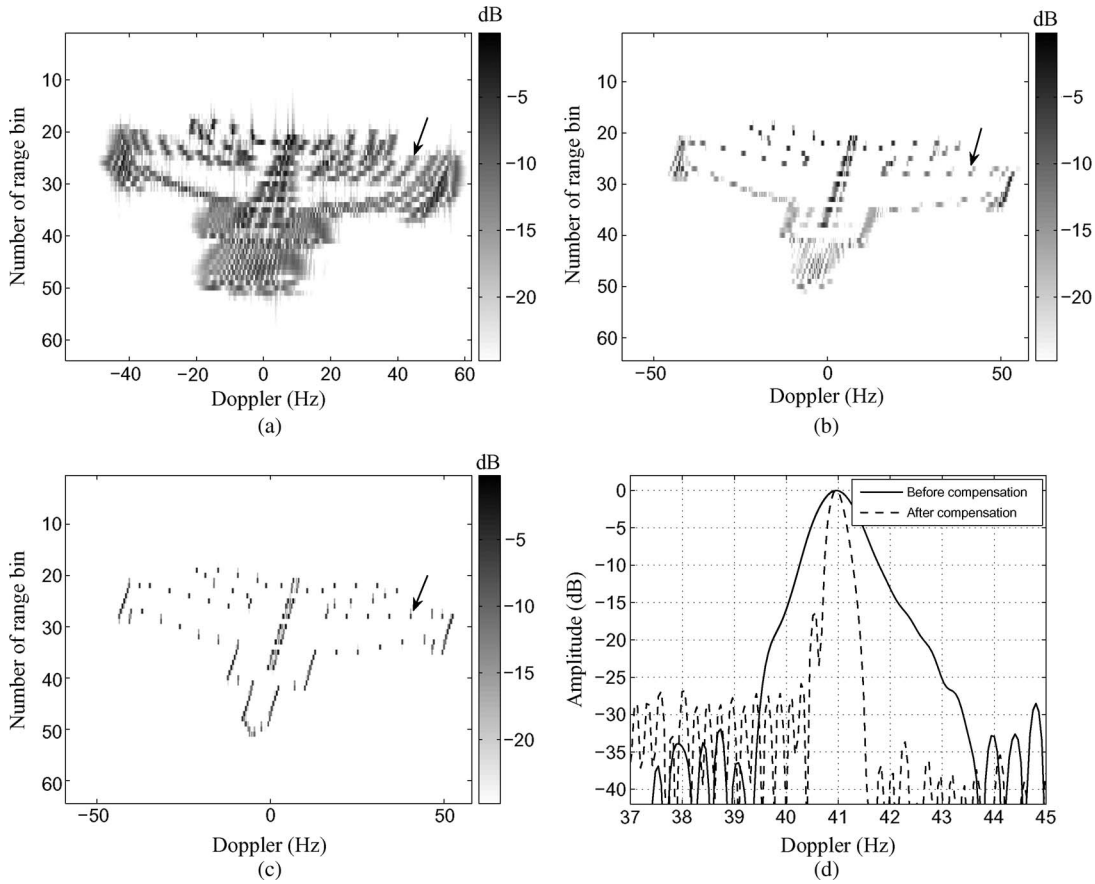

Fig. 3. ISAR images for the simulated data. (a) Using the standard technique RDA. (b) Using the RID algorithm without previous motion compensation (ISAR image corresponding to $CPI/2$ s). (c) Applying motion compensation prior to the RID algorithm (ISAR image corresponding to $CPI/2$ s). (d) Doppler cutoffs of the PSF of the indicated target scatterer.

III. Mitigation of Doppler Spreading

As shown above, the cause of the quality degradation (Doppler spreading) is the migration in slant range of the scatterers. Not only the translational motion but also the rotational motion may induce migrations in slant range.

Consequently, a complete previous motion compensation guarantees that each scatterer remains in its corresponding range bin during the CPI, which means that this compensation prior to the RID processing (Fig. 1) provides us with mitigation of the Doppler spreading of the scatterers PSF in each of the obtained ISAR images.

Motion compensation may be divided into translational and rotational motion compensation stages. The first one is implemented in this letter as follows.

1) The range bin alignment step is implemented by using the extended envelope correlation method [8]. This technique uses reference profiles to minimize the error accumulation effect and makes fractional alignment via optimization. The method is robust against target scintillation, noise and clutter [8].
2) Improved entropy minimization [14] is employed for the phase adjustment step. The method is nonparametric and computationally more efficient than the trial-and-error approach [13].

For the rotational motion compensation stage, several methods may be used [17]–[22]. Here, we employ slant-range rotation compensation and cross-range rotation compensation [27], which are valid for uniform rotational rates. In case of complex motions of noncooperative maneuvering targets, where even the direction of the effective rotation vector may quickly change, we admit that the rotational motion compensation may be very difficult or even impossible [28]. For these cases, it is interesting, at least, to compensate the translational motion prior to the RID processing. Thus, the Doppler spreading effect may be greatly mitigated.

IV. Results

A. Simulated Data

Simulated data have been used to confirm the existence of Doppler spreading when using the RID technique. The simulated example has extensively been used in the literature for comparison purposes [29]. The data belong to a simulated MIG-25 aircraft composed of 120 scatterers. The target is uniformly rotating, while a stepped frequency radar illuminates it. The central frequency is 9 GHz, the number of stepped frequencies in a burst is 64, the pulse repetition frequency is 15 000 Hz, the total number of bursts is 512 and the synthesized bandwidth is 512 MHz.

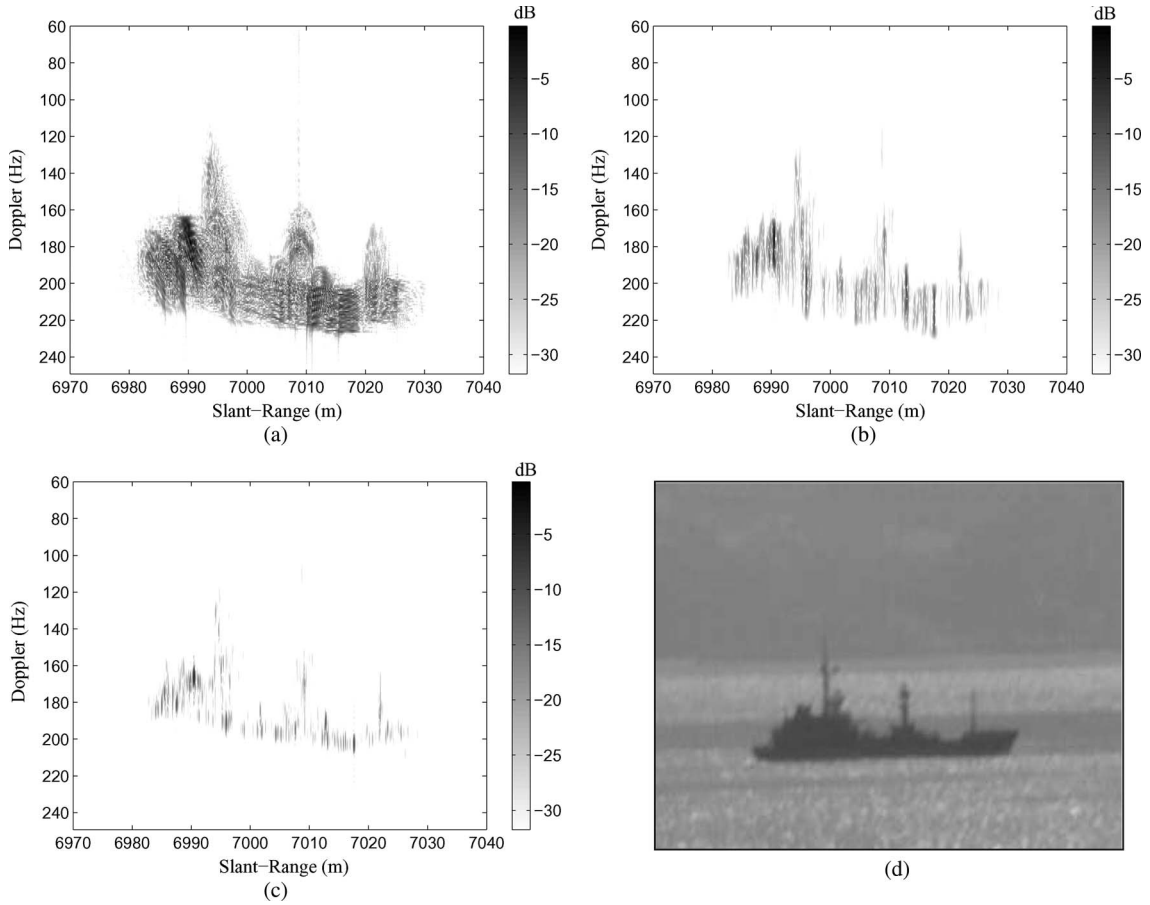

Fig. 4. ISAR images of the live capture and photograph of the vessel. (a) Using the standard technique RDA. (b) Using the RID algorithm without previous motion compensation (ISAR image corresponding to $CPI/2$ s). (c) Applying motion compensation prior to the RID algorithm (ISAR image corresponding to $CPI/2$ s). (d) Photograph of the vessel.

Fig. 3(a) shows the ISAR image obtained with the standard RDA. Note that target rotation generates space-variant slant-range migration for the target scatterers. The ISAR image, corresponding to $CPI/2$ s, obtained by the RID technique without previous motion compensation is shown in Fig. 3(b), whereas Fig. 3(c) shows the analogous result when motion has been compensated prior to the RID technique. The SPWVD has been used as TFT for both cases. An arrow in Figs. 3(a)–(c) marks a target scatterer with slant-range migration. Fig. 3(d) shows the Doppler cutoffs of the PSF of this scatterer for Fig. 3(b) and (c). As expected, Fig. 3(c) is more focused than Fig. 3(b). The PSF Doppler width at -3-dB points is 0.76 and 0.29 Hz for the indicated scatterer in Fig. 3(b) and (c), respectively. Clearly, the slant-range migration induced by the rotational motion indirectly causes Doppler spreading by applying the RID technique without a previous motion compensation.

B. Real Data

Real data from a vessel have also been used to confirm the given analysis and to validate the approach. The ship was illuminated by a millimeter-wave linear frequency-modulated continuous-wave radar [30] for a CPI of 1.27 s. The central frequency is 28.5 GHz, the transmitted bandwidth is 1 GHz, and the pulse repetition frequency is 500 Hz. The acquisition campaign was made in the Strait of Gibraltar.

Fig. 4(a) shows the ISAR image obtained with the standard processing RDA. The image is blurred not only in Doppler but also in slant range. Fig. 4(b) shows the ISAR image, corresponding to $CPI/2$ s, after using the RID technique without previous motion compensation. The SPWVD has been used as TFT. On the other hand, Fig. 4(c) shows the analogous result using the RID technique when motion has previously been compensated. As expected, Doppler spreading is noticeable in Fig. 4(b), whereas it has greatly been reduced in Fig. 4(c). A photograph of the vessel is shown in Fig. 4(d) for reference.

V. Conclusion

The direct application of the RID technique to generate a sequence of ISAR images may produce Doppler spreading of the PSF of the target scatterers. In this letter, it has been shown that the reason of this blurring is found in the migration of the scatterers in slant range. In order to mitigate this Doppler spreading, motion compensation must be applied prior to the TFT-based processing. This motion compensation should guarantee that the target scatterers remain in their corresponding range bins during the CPI. Both simulated and real data have allowed us to verify the analysis and to check the convenience of applying the mitigation technique.

ACKNOWLEDGMENT

The authors would like to thank Dr. V. C. Chen for providing the simulation data and Dr. A. Blanco-del-Campo, Dr. A. Asensio-López, and Dr. B. P. Dorta-Naranjo for providing the live data of the ship. The authors would also like to thank the reviewers for the provided feedback.

REFERENCES

[1] C. C. Chen and H. C. Andrews, "Target motion induced radar imaging," *IEEE Trans. Aerosp. Electron. Syst.*, vol. AES-16, no. 1, pp. 2–14, Jan. 1980.

[2] D. A. Ausherman, A. Kozma, J. L. Walker, H. M. Jones, and E. C. Poggio, "Developments in radar imaging," *IEEE Trans. Aerosp. Electron. Syst.*, vol. AES-20, no. 4, pp. 363–400, Jul. 1984.

[3] S. A. Hovanessian, *Introduction to Sensor Systems*. Boston, MA: Artech House, 1988.

[4] A. V. Jelalian, *Laser Radar Systems*. Boston, MA: Artech House, 2002.

[5] D. R. Wehner, *High-Resolution Radar*. Boston, MA: Artech House, 1995.

[6] J. L. Walker, "Range-Doppler imaging of rotating objects," *IEEE Trans. Aerosp. Electron. Syst.*, vol. AES-16, no. 1, pp. 23–52, Jan. 1980.

[7] G. Y. Delisle and H. Wu, "Moving target imaging and trajectory computation using ISAR," *IEEE Trans. Aerosp. Electron. Syst.*, vol. 30, no. 3, pp. 887–899, Jul. 1994.

[8] J. M. Muñoz-Ferreras and F. Pérez-Martínez, "Extended envelope correlation for range bin alignment in ISAR," in *Proc. IET Conf. Radar Syst.*, Oct. 2007, pp. 1–5.

[9] T. Itoh, H. Sueda, and Y. Watanabe, "Motion compensation for ISAR via centroid tracking," *IEEE Trans. Aerosp. Electron. Syst.*, vol. 32, no. 3, pp. 1191–1197, Jul. 1996.

[10] J. Wang and D. Kasilingam, "Global range alignment for ISAR," *IEEE Trans. Aerosp. Electron. Syst.*, vol. 39, no. 1, pp. 351–357, Jan. 2003.

[11] B. D. Steinberg, "Microwave imaging of aircraft," *Proc. IEEE*, vol. 76, no. 12, pp. 1578–1592, Dec. 1988.

[12] D. E. Wahl, P. H. Eichel, D. C. Ghiglia, and C. V. Jakowatz, Jr., "Phase gradient autofocus—A robust tool for high resolution SAR phase correction," *IEEE Trans. Aerosp. Electron. Syst.*, vol. 30, no. 3, pp. 827–835, Jul. 1994.

[13] X. Li, G. Liu, and J. Ni, "Autofocusing of ISAR images based on entropy minimization," *IEEE Trans. Aerosp. Electron. Syst.*, vol. 35, no. 4, pp. 1240–1252, Oct. 1999.

[14] J. Wang, X. Liu, and Z. Zhou, "Minimum-entropy phase adjustment for ISAR," *Proc. Inst. Elect. Eng.—Radar, Sonar Navig.*, vol. 151, no. 4, pp. 203–209, Aug. 2004.

[15] M. Martorella, F. Berizzi, and B. Haywood, "Contrast maximisation based technique for 2-D ISAR autofocusing," *Proc. Inst. Elect. Eng.—Radar, Sonar Navig.*, vol. 152, no. 4, pp. 253–262, Aug. 2005.

[16] Z. She and Y. Liu, "Autofocus for ISAR imaging using higher order statistics," *IEEE Geosci. Remote Sens. Lett.*, vol. 5, no. 2, pp. 299–303, Apr. 2008.

[17] S. Werness, W. Carrara, L. Joyce, and D. Franczak, "Moving target imaging algorithm for SAR data," *IEEE Trans. Aerosp. Electron. Syst.*, vol. 26, no. 1, pp. 57–67, Jan. 1990.

[18] R. Lipps and D. Kerr, "Polar reformatting for ISAR imaging," in *Proc. Nat. Radar Conf.*, May 1998, pp. 275–280.

[19] J. M. Muñoz-Ferreras and F. Pérez-Martínez, "Non-uniform rotation rate estimation for ISAR in case of slant range migration induced by angular motion," *IET Radar, Sonar Navig.*, vol. 1, no. 4, pp. 251–260, Aug. 2007.

[20] M. Xing, R. Wu, J. Lan, and Z. Bao, "Migration through resolution cell compensation in ISAR imaging," *IEEE Geosci. Remote Sens. Lett.*, vol. 1, no. 2, pp. 141–144, Apr. 2004.

[21] I. Djurovic, T. Thayaparan, and L. J. Stankovic, "Adaptive local polynomial Fourier transform in ISAR," *J. Appl. Signal Process.*, vol. 1, pp. 1–15, 2006.

[22] L. Du and G. Su, "Adaptive inverse synthetic aperture radar imaging for nonuniformly moving targets," *IEEE Geosci. Remote Sens. Lett.*, vol. 2, no. 3, pp. 247–249, Jul. 2005.

[23] V. C. Chen and H. Ling, *Time–Frequency Transforms for Radar Imaging and Signal Analysis*. Norwood, MA: Artech House, 2002.

[24] Z. Bao, C. Sun, and M. Xing, "Time–frequency approaches to ISAR imaging of maneuvering targets and their limitations," *IEEE Trans. Aerosp. Electron. Syst.*, vol. 37, no. 3, pp. 1091–1099, Jul. 2001.

[25] F. Berizzi, E. D. Mese, M. Diani, and M. Martorella, "High-resolution ISAR imaging of maneuvering targets by means of the range instantaneous Doppler technique: Modeling and performance analysis," *IEEE Trans. Image Process.*, vol. 10, no. 12, pp. 1880–1890, Dec. 2001.

[26] O. Rioul and P. Flandrin, "Time-scale energy distributions: A general class extending wavelet transforms," *IEEE Trans. Signal Process.*, vol. 40, no. 7, pp. 1746–1757, Jul. 1992.

[27] J. M. Muñoz-Ferreras and F. Pérez-Martínez, "Uniform rotational motion compensation for inverse synthetic aperture radar with noncooperative targets," *IET Radar, Sonar Navig.*, vol. 2, no. 1, pp. 25–34, Feb. 2008.

[28] A. W. Rihaczek and S. J. Hershkowitz, *Theory and Practice of Radar Target Identification*. Norwood, MA: Artech House, 2000.

[29] V. C. Chen, 1999. [Online]. Available: http://airborne.nrl.navy.mil/~vchen/tftsa.html

[30] A. Blanco del Campo, A. Asensio López, B. Pablo Dorta Naranjo, J. Gismero Menoyo, D. Ramirez Morán, C. Carmona Duarte, and J. L. Jiménez Martín, "Millimeter-wave radar demonstrator for high resolution imaging," in *Proc. 1st Eur. Radar Conf.*, Oct. 2004, pp. 65–68.